ELSEVIER

Journal of Nuclear Materials 305 (2002) 187–201

journal of nuclear materials

www.elsevier.com/locate/jnucmat

Plutonium chemistry: a synthesis of experimental data and a quantitative model for plutonium oxide solubility

J.M. Haschke [a], V.M. Oversby [b,*]

[a] *Actinide Sciences Consulting, 1103 Willow Bend Drive, Waco, TX 76712, USA*
[b] *VMO Konsult, Karlavägen 70, SE-114 59 Stockholm, Sweden*

Received 2 May 2002; accepted 9 July 2002

Abstract

The chemistry of plutonium is important for assessing potential behavior of radioactive waste under conditions of geologic disposal. This paper reviews experimental data on dissolution of plutonium oxide solids, describes a hybrid kinetic-equilibrium model for predicting steady-state Pu concentrations, and compares laboratory results with predicted Pu concentrations and oxidation-state distributions. The model is based on oxidation of PuO_2 by water to produce PuO_{2+x}, an oxide that can release Pu(V) to solution. Kinetic relationships between formation of PuO_{2+x}, dissolution of Pu(V), disproportionation of Pu(V) to Pu(IV) and Pu(VI), and reduction of Pu(VI) are given and used in model calculations. Data from tests of pyrochemical salt wastes in brines are discussed and interpreted using the conceptual model. Essential data for quantitative modeling at conditions relevant to nuclear waste repositories are identified and laboratory experiments to determine rate constants for use in the model are discussed.

1. Introduction

Radioactive wastes with significant concentrations of plutonium are produced by civilian nuclear reactors and by military activities. Disposal of these wastes in geologic repositories requires an understanding of the behavior of Pu in the waste forms and in solutions that interact with those waste forms. Pyrochemical salt residues from the purification of weapons-grade Pu at the Rocky Flats Plant in Colorado are a high-Pu waste that is already being disposed of at the Waste Isolation Pilot Plant (WIPP) facility in New Mexico. The focus of this paper is on development of a model for dissolution of plutonium oxide in near-neutral solutions and on data needed to allow application of the model to Rocky Flats salt wastes under conditions relevant for WIPP.

Plutonium solution chemistry has been studied primarily under conditions of low pH in the development of separations procedures used in production and purification of military Pu. Acidic conditions are also used for separation of Pu from the other components of spent nuclear fuel during preparation of mixed U–Pu dioxide (MOX) nuclear fuel. Studies of plutonium chemistry in solutions with near-neutral pH, which are most relevant for waste disposal conditions, have been limited. In near-neutral pH solutions, the solubility of Pu is very low, which leads to difficulties making measurements of solution concentrations and speciation of Pu in the solutions. Plutonium also presents difficulties because it is capable of existing in a number of different valence states and of having different valence states in the solid phase(s) and in the coexisting solution.

The discovery of a plutonium oxide phase, PuO_{2+x}, with higher oxygen content than PuO_2 [1] suggests that the dioxide is not stable under all conditions in the environment and that reevaluation of plutonium observational and experimental data might account for many results that previously had seemed inconsistent. Results

---

[*] Corresponding author. Tel.: +46-8 667 2645; fax: +46-8 661 5782.
E-mail address: virginia.oversby@stockholm.mail.telia.com (V.M. Oversby).

0022-3115/02/$ - see front matter © 2002 Elsevier Science B.V. All rights reserved.
PII: S0022-3115(02)00922-4

of a recent assessment indicate that the widely accepted solubility model fails to account for dissolution behavior of plutonium oxide in controlled laboratory studies [2]. Plutonium chemistry and the importance of kinetics in controlling steady-state concentrations of plutonium species in solutions are summarized in Section 2. Conceptual and quantitative models developed from kinetic and equilibrium thermodynamic data are presented in Section 3.

Development of safe disposal systems for Pu-containing wastes requires understanding the possible behavior of the waste materials and their components under a variety of conditions and in contact with diverse aqueous media. Use of a hybrid kinetic-equilibrium model in predicting steady-state concentrations and valence-state distributions of Pu in low-ionic-strength solutions and brines at near-neutral pH is discussed. Data presently available for performance predictions of pyrochemical salt wastes are summarized. Recommendations are given for new studies that would improve the ability of repository designers and operators to evaluate the long-term behavior of these waste materials.

2. Plutonium chemistry

Understanding the behavior of plutonium under storage conditions is important for maintenance of safety in storage facilities prior to waste disposal. Some materials, such as pyrochemical salts, have been stored under a variety of conditions prior to disposal. In this overview, we discuss some Pu-containing materials of interest and reactions that those materials might undergo. Specifically, we discuss the reactions of metallic Pu with air, oxygen, and water. Products of these reactions have various compositions and in turn can react with air and/or water to form other products that also influence dissolution behavior.

2.1. Oxidation of plutonium metal

The rates and products of reaction between Pu metal and air, oxygen, and water are described in a series of reports [3–10]. In the presence of air or oxygen, a fresh Pu metal surface rapidly becomes covered with a layer of PuO_2. The dioxide is a ‘protective’ layer because it controls the rate of further oxidation by limiting the rate of oxygen diffusion to the product–metal interface [9,10]. As oxidation/corrosion proceeds, the thickness of the oxide diffusion barrier increases according to a parabolic rate law over time. When the layer becomes sufficiently thick, stress-induced spallation of oxide begins and more rapid oxidation occurs in thin regions. Thereafter, the Pu surface is covered by a microscopically uneven PuO_2 layer with a constant average thickness maintained by continuing spallation and oxidation. Spallation is accompanied by a kinetic regime in which time dependence of oxidation is linear and the rate is constant. In water vapor or moist air, the oxidation rate at room temperature is increased by more than 100 fold [6]. Rate enhancement is attributed to formation of PuO_{2+x} at the gas–solid interface, a process that increases the gradient in oxygen concentration across the diffusion barrier [5,9].

If Pu metal survives the storage conditions without oxidation, exposure to natural waters in the repository results in production of oxide via a complex sequence of reactions [1,4]. The initial compound formed by the Pu–water reaction is plutonium monoxide monohydride (PuOOH). In sequential oxidation steps, water reacts to form a second oxide hydride ($Pu_7O_9H_3$), Pu_2O_3, members of the Pu_nO_{2n-1} homologous series ($n = 7$, 9, 10, 12), PuO_2, and PuO_{2+x}. All products apparently have fluorite-related structures with fcc lattices of Pu cations. Reaction at room-temperature proceeds initially as hydride (H^-) in a lattice of Pu(III) ions is replaced by oxide (O^{2-}) and subsequently as additional oxygen is accommodated on vacant lattice sites as oxide. This process results in progressive oxidization of Pu from Pu(III) to Pu(IV) and Pu(V) [1,4]. This reaction series is important in interpreting test results for pyrochemical salt residues in brines.

2.2. Reaction of plutonium dioxide

CaF_2-type PuO_2 is a well characterized crystalline solid, but the distinction between the dioxide and the amorphous tetrahydroxide, $Pu(OH)_4$ (am), formed by precipitation of Pu^{4+} from aqueous solution is often blurred. Tetrahydroxide is also identified in the literature as hydrous oxide ($PuO_2 \cdot 2H_2O$) and as PuO_2 (am), implying properties like those of dioxide. Thermodynamic data [11] and experimental observation [12] show that the $Pu(OH)_4$ precipitate is metastable and transforms into crystalline PuO_2. Disproportionation of $Pu(OH)_4$ (s) into dioxide and water at 25 °C is driven by a ΔG^0 of −40 kJ/mol. Metastable tetrahydroxide is more soluble than dioxide and Pu concentrations, [Pu], of solutions in equilibrium with $Pu(OH)_4$ should decrease over time as hydroxide transforms into crystalline oxide.

Early studies of plutonium chemistry indicated that PuO_2 does not react with oxygen, ozone, or nitrogen dioxide. These observations were interpreted as evidence that oxides with compositions higher than PuO_2 are unstable and do not form [13–15]. Evidence for the formation of a higher oxide was initially found at the gas–solid interface during corrosion of Pu in water vapor [5]. This phase is confirmed by more recent studies showing that exposure of PuO_2 to H_2O results in H_2 production and a concurrent mass gain consistent with stoichiometric incorporation of oxygen in the oxide

[1,2,7,8]. Reaction of dioxide with water at room temperature and with water vapor at 25–350 °C produces the higher oxide according to the reaction

$$PuO_2\ (s) + xH_2O\ (l, g) \rightarrow PuO_{2+x}\ (s) + xH_2\ (g). \quad (1)$$

The rate, R, of Eq. (1) is temperature dependent, indicating that the process is chemical, not radiolytic [1].

$$\ln R(\mathrm{mol\,H_2O/m^2\,h}) = -6.441 - (4706/T). \quad (2)$$

This equation and experimental uncertainties in the rate at room temperature, give a value of R of $2.2 \pm 1.4 \times 10^{-10}$ (mol H_2O/m^2 h) for the reaction in low-ionic-strength solutions and chloride-rich (1 m $CaCl_2$) brine at 25 °C. Production of oxidants due to the radiolysis of H_2O adsorbed on $^{239}PuO_2$ is indicated by the rate of radiolytic H_2 formation for these conditions. The hydrogen production rate based on the molecular yield (G_{H2}) for alpha radiolysis of liquid water is $9 \pm 4 \times 10^{-12}$ mol/m^2 h [16]. The observed reaction rate exceeds the maximum oxidation rate due to radiolytic products by a factor of about 30 at 25 °C and by about 10^5 at 350 °C. The difference between the observed rate and radiolytic rates increases with temperature because radiolysis is not a function of temperature. These observations support a chemical origin for the oxidation process.

Formation of higher oxide is not observed if dioxide is exposed to dry air or O_2, but occurs in the presence of moisture [1]. As shown by the rate of O_2 consumption, PuO_{2+x} is produced at the rate characteristic of the PuO_2–H_2O reaction, but H_2 is not formed. Behavior is consistent with a water-catalyzed cycle comprised of three steps:

$$PuO_2(s) + xH_2O\ (ads) \rightarrow PuO_{2+x}\ (s) + 2xH\ (ads), \quad (3)$$

$$(x/2)O_2\ (g) = xO\ (ads), \quad (4)$$

$$2xH\ (ads) + xO\ (ads) \rightarrow xH_2O\ (ads), \quad (5)$$

$$PuO_2\ (s) + (x/2)O_2\ (g) \rightarrow PuO_{2+x}\ (s). \quad (6)$$

In the absence of O_2, H atoms formed via Eq. (3) associate with release of H_2 according to Eq. (1). The rapid rate of PuO_{2+x} formation by water compared to O_2 is attributed to chemisorption of H_2O as OH^- and facile transformation of OH^- into O^{2-} [9]. Whereas O^{2-} formation by dissociatively adsorbed oxygen is a low-probability process requiring transfer of two electrons, formation of oxide by hydroxide is a relatively facile one-electron process. The reaction path of Eqs. (3)–(5) provides an explanation for initial 'implosion' of sealed storage cans containing PuO_2(s) and air as moisture-catalyzed reaction consumes oxygen in the storage atmosphere [16].

X-ray diffraction data for solid products of the PuO_2–H_2O reaction show a single CaF_2-related phase with a lattice parameter that increases by 0.4 pm as reaction initiates [1]. Linear variation of the cubic parameter with PuO_{2+x} composition, a_0 (nm) $= 0.53643 + 0.001764(2 + x)$, is consistent with formation of an extended solid solution similar to UO_{2+x}. Excess oxygen is apparently accommodated on octahedral interstices of the PuO_2 lattice. Self-induced radiation damage does not account for the observed increase in a_0 [17]. Although initial X-ray photoelectron data suggested that Pu(IV) is progressively replaced by Pu(VI) as x increases [5], subsequent extended X-ray absorption fine structure results show substitution of Pu(V) [18], implying that the solid solution is described by the formula $Pu(IV)_{1-2x}$-$Pu(V)_{2x}O_{2+x}$. Although experimental data show that the value of x in PuO_{2+x} extends to 0.27, the maximum value of x has not been experimentally determined [1]. Extension of x to 0.5 is expected on the basis of the general formula. Stability of PuO_{2+x} is supported by a thermodynamic assessment indicating that ΔG_f^0 decreases from −998 to −1146 kJ/mol and the equilibrium O_2 pressure increases from 10^{-133} to10^{-83} bar as x increases from 0 to 0.5 [17].

Identification of PuO_{2+x} provides rational explanations for perplexing observations in the descriptive chemistry of Pu. Divergent reports that PuO_2 may be either green or dull yellow to khaki in color [13] are addressed by the observation that PuO_{2+x} is consistently green [1]. Whereas so-called 'high-fired' oxide formed by calcination above 800 °C is difficult to dissolve, 'low-fired' dioxide prepared at 400–500 °C dissolves rather easily [11]. Thermodynamic estimates indicate that $PuO_{2.2}$ is the equilibrium oxide in air at low firing temperatures [17] and analogy to the uranium–oxygen system suggests that oxide solubility is increased by high-oxidation-state cations [19]. Formation of PuO_{2+x} in air, in water vapor, and in near-neutral salt solution under 1.5 bar H_2 [1,4] implies that the higher oxide is stable in the environment and that oxide solubility may be enhanced by its formation.

2.3. Solution chemistry of plutonium oxide

2.3.1. Steady-state solutions

Plutonium concentrations measured at steady state during dissolution studies with PuO_2 and $Pu(OH)_4$ solids over a wide range of conditions depend on pH as shown in Fig. 1. Results for $Pu(OH)_4$ (am) (solid symbols) are for initially oversaturated and undersaturated conditions with atmospheres of air or Ar–1.57% CO_2 and ionic strengths ranging from 10^{-7} to 3 molal [20–25]. The data set for $Pu(OH)_4$ includes results from studies in which plutonium was added to the solution as $Pu(OH)_4$ (am), solid colloidal hydroxide, Pu^{3+} (aq), Pu^{4+} (aq), PuO_2^+, and PuO_2^{2+}. Open symbols are for crystalline

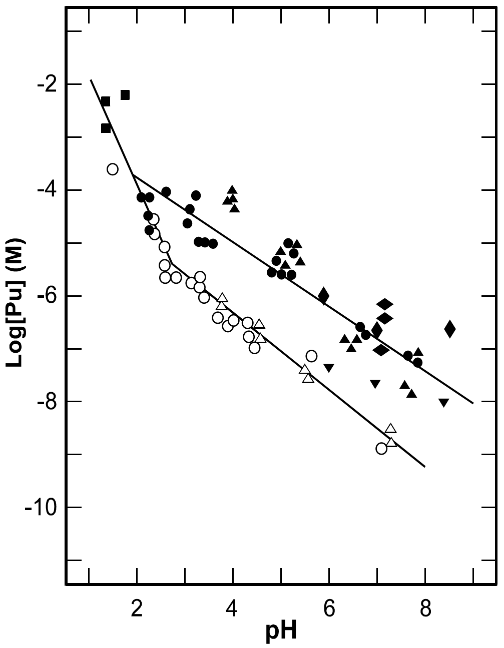

Fig. 1. Dependence of the steady-state [Pu] on pH from dissolution studies with PuO_2 (s) (open symbols) and $Pu(OH)_4$ (am) (solid symbols) in differing atmospheres and solutions. Data are derived form literature sources as follows: horizontal diamonds [20], upright triangles [21], circles [22], squares, [23], vertical diamonds [24], and inverted triangles [25].

PuO_2 in low-ionic-strength solutions exposed to air [21,22]. Data are described by a single regression line for the region with $pH < 2.5$ and by separate lines for the two solids at higher pH [2]. The slope for $pH < 2.5$ is -2.1 ± 0.4 and slopes for PuO_2 and $Pu(OH)_4$ are -0.73 ± 0.03 and -0.59 ± 0.04, respectively. Recent measurements for hydroxide in 0.4 M $NaClO_4$ and NaCl solutions at pH 4–9 gave slopes near −0.8, confirming the earlier results [26]. As concluded in that study, a slope near −1 is consistent with dissolution of Pu(V) as PuO_2^+. These observations do not agree with the zero slope expected for formation of $Pu(OH)_4$ (aq) during dissolution of Pu(IV) at $pH > 5$ [2].

Steady-state Pu concentrations from studies with $Pu(OH)_4$ (am) in Fig. 1 lie in a band with a width of about two orders of magnitude and are consistently higher than [Pu] for crystalline PuO_2 at $pH > 3$. Insensitivity of steady-state [Pu] to chemical potential (*Eh*) and to ionic strength (*I*) is implied by this limited range [2]. The observed difference in apparent solubility for hydroxide and dioxide is about 10^2. Thermodynamic modeling predicts an equilibrium [Pu] for the crystalline solid of approximately 10^{-17} M [25] and independent calculations confirm a difference of 10^8 between equilibrium concentrations for dioxide and hydroxide [2].

The small difference between the observed steady-state [Pu] of PuO_2 and that of $Pu(OH)_4$ has been attributed to enhancement of oxide solubility by formation of hydroxide on the PuO_2 surface in water [27]. Dissociative chemisorption of H_2O at 25 °C and pressures below 0.3 mbar transforms the surface composition to $PuO(OH)_2$, which becomes more stable as water activity increases [28]. It is most unlikely, however, that this limited surface reaction could explain an increase in solubility for the solid of 8 orders of magnitude over that calculated based on thermodynamic properties data. Hydration of the surface is the first step in most dissolution mechanisms for solids and does not result in significant differences between measured and predicted solubilites in general.

Dissolution studies have been conducted with the solid product removed from a test with crystalline PuO_2 at pH 1.5 [22]. Log[Pu] values measured after placing the recovered solid in new solutions at pH 4.3 and 4.8 were −5.3 and −4.8, respectively. These steady-state Pu concentrations correspond to values associated with $Pu(OH)_4$ (am), not to those of PuO_2 [2]. These results seem to imply that crystalline PuO_2 transformed into amorphous $Pu(OH)_4$, a process that violates thermodynamic constraints, unless hydroxide is more stable than dioxide in acidic media. The observations are consistent, however, with transformation of both dioxide and hydroxide into a solid that is both more stable and more soluble than PuO_2.

As shown in a review of results from dissolution studies with PuO_2 (s) and $Pu(OH)_4$ (am) [2], the predominant oxidation states of Pu at steady state in laboratory experiments and in natural waters at pH 1–9 are consistently Pu(V) and Pu(VI). Studies with hydroxide in water from the Yucca Mountain region at pH 5.9–8.5 show 0.1–6% Pu(IV), 39–73% Pu(V), and 18–59% Pu(VI) [20,29]. Similar studies with $Pu(OH)_4$ in simulated WIPP brine at pH 7.1 and exposed to an atmosphere with 21% O_2 and 0.26% CO_2 show 1–5% Pu(IV), 5–28% Pu(V), and 70–96% Pu(VI) [24]. The oxidation-state distribution obtained with crystalline PuO_2 microspheres in 1 mM $NaHCO_3$ solution at pH 7 is 5% Pu(IV), no detectable Pu(V), and 95% Pu(VI) [30]. During studies with PuO_2 (am), Rai et al. [26] determined that Pu(V + VI) is the dominant Pu fraction in air-exposed steady-state solutions at $pH > 3.4$ using a solvent extraction method that could not distinguish between Pu(V) and Pu(VI). In an interpretation of spent fuel dissolution data, Choppin [31] proposed that the solution species is PuO_2^+, while the solubility-controlling solid is $Pu(OH)_4$. Observed oxidation states at steady state are inconsistent with the behavior of an equilibrium system; the calculated distribution in air-saturated pH 7 solution ($Eh = 0.80$ V) coexisting with PuO_2 or $Pu(OH)_4$ is 0.0% Pu(IV), 96.1% Pu(V) and 3.9% Pu(VI) [2].

Electrochemical potentials measured at steady state in studies with PuO_2 and $Pu(OH)_4$ in solutions exposed to air and Ar–1.75% CO_2 at pH 4–8 [21,24,25] are described by a single linear *Eh*–pH equation [2].

$$Eh\ (V) = 0.74 \pm 0.02 - (0.0596 \pm 0.0035)pH. \qquad (7)$$

Although of uncertain reliability, *Eh* corresponds to a constant oxygen activity of about 10^{-33} bar O_2 for both starting solids. Calculated equilibrium Pu concentrations and oxidation state distributions at *Eh*–pH values defined by Eq. (7) do not account for observed behavior [2]. For a solution with $Pu(OH)_4$ (am) at pH 7 ($Eh = 0.32$ V), the predicted equilibrium log[Pu] is −8.8 and Pu(IV) accounts for more than 99.99% of the Pu in solution. Insensitivity of the measured potential to gas atmosphere and the surprisingly low voltages of air-exposed solutions suggest that either the measured values are substantially in error or that the measured *Eh* is not for the redox couple involved in the expected reaction(s) of plutonium.

Insight into the observed behavior is gained by the comparison of pH dependencies of steady-state log[Pu] (solid symbols) and *Eh* (open symbols) from studies with $Pu(OH)_4$ by Rai and coworkers in Fig. 2. Data at low pH (triangles) [32] and intermediate pH (circles) [21] are for air-exposed HNO_3 solutions and those at high pH (squares) are for KOH solutions in which low O_2 concentrations were maintained by careful procedures [33].

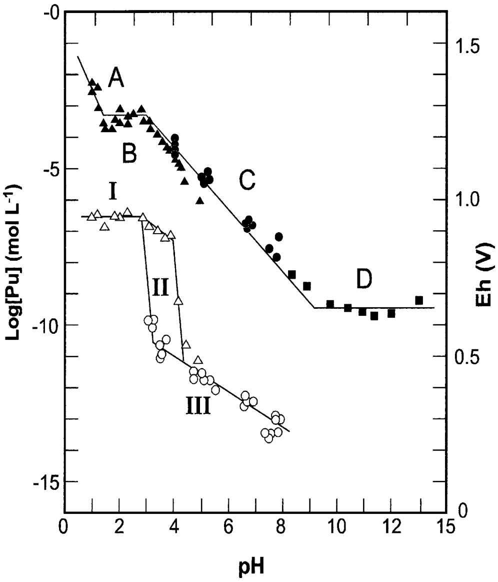

Fig. 2. The pH dependencies of steady-state [Pu] (solid symbols) and *Eh* (open symbols) from dissolution studies with $Pu(OH)_4$ (am) in low-ionic-strength solutions. Data are from literature sources as follows: upright triangles [21], circles [32], and squares [33].

Four regions (A–D) are evident in the log[Pu]–pH data with data in Region C described by the ideal slope of −1 for the pH 3–9 range. The slope in Region A is −2 and slopes in Regions B and D are near zero. Termination of Region C near pH 3 coincides with a sharp increase of about 0.4 V indicated by Region II in the *Eh* data. *Eh* values near 0.95 V in Region I are consistent with values for air-exposed solutions, suggesting that the measurements were reasonably accurate. Potentials in Region III are described by a line with a theoretical slope of 0.059, but are surprisingly low for air-exposed solutions. Correspondence of Regions C and III suggests that low *Eh* values are characteristic of the region with −1 slope for log[Pu] versus pH.

Another unanticipated result for steady-state solutions is a dependence of plutonium concentrations on the amount of solid present in the system [2]. Equilibrium expressions derived from spectroscopic data are reported for steady-state solutions at pH 1–2 [23]. Steady-state solutions formed after addition of colloidal Pu(IV), Pu(V) (aq), or Pu(VI) (aq) contained no detectable oxidation states other than Pu(V) and Pu(VI). The apparent equilibrium system is defined by disproportionation of Pu(V) and precipitation of solid hydroxide or hydrous oxide.

$$2PuO_2^+\ (aq) + 2H_2O \rightarrow PuO_2^{2+}\ (aq) + Pu(OH)_4\ (am). \qquad (8)$$

Measured equilibrium expressions ($K = [PuO_2^{2+}]/[PuO_2^+]^2$) vary systematically by 10^3 with the moles of Pu-containing solid in contact with the solution [2]. In addition to conflicting with the fundamental principle of equilibrium, this behavior implies that the distribution of Pu(V) and Pu(VI) also depends on the amount of solid present.

2.3.2. Steady-state solids

Results of XRD measurements on steady-state solids formed during dissolution studies lead Rai and Ryan [22] to conclude that chemical and radiolytic effects transform PuO_2 and $Pu(OH)_4$ into a less crystalline solid with properties between those of crystalline dioxide and freshly prepared amorphous hydroxide. Evaluation of crystallographic data [2,17] for CaF_2-related products formed by PuO_2 [22] and by $Pu(OH)_4$ [34] yield cubic lattice parameters that significantly exceed a_0 of PuO_2. Increases in a_0 are within the range of self-irradiation damage [35], but all observations are not accounted for by that process [17]. An alternative interpretation of the observations is that the steady-state products are PuO_{2+x}. Derived lattice parameters and the a_0–x relationship in Section 2.2 show that a_0 values of solids formed at pH 7 ($a_0 = 0.5404$) and near pH 3 ($a_0 = 0.541$ nm) correspond to $PuO_{2.27}$ and $PuO_{2.5}$, respectively.

2.3.3. Dissolution kinetics

A review of dissolution studies involving oversaturation of natural and laboratory waters with Pu^{4+} (aq) shows that precipitation of $Pu(OH)_4$ (am) is not followed by the anticipated decrease in [Pu] as hydroxide transforms into dioxide [2]. Over a period of weeks, pH values of near-neutral waters from the Yucca Mountain region [20] and synthetic WIPP brine [24] remain constant, but Pu concentrations progressively increase to steady-state values that exceed the equilibrium [Pu] for $Pu(OH)_4$ (am) by more than 10^2. Observations are inconsistent with solubility control by hydroxide and suggest that hydroxide transforms into a more soluble solid than $Pu(OH)_4$ (am).

Measurements of dissolution rates in studies with PuO_2 in distilled water and normal saline solution at 37 °C show that values approach a steady state after ≈ 1 y [36]. The average area-normalized rate derived from data for crystalline $^{239}PuO_2$ at steady state is $(2 \pm 1) \times 10^{-8}$ mol Pu/m^2 d. The rate of Pu(V) formation in PuO_{2+x} at 37 °C is 1.9×10^{-8} mol Pu/m^2 d, a value twice the rate of H_2 formation calculated using Eq. (2). Coincidence of the Pu(V) formation rate with the dissolution rate suggests that PuO_{2+x} is involved in dissolution of plutonium as Pu(V) and that steady-state Pu concentrations are kinetically controlled.

2.3.4. Disproportionation kinetics

Persistent appearance of pentavalent plutonium in steady-state solutions together with its well-known disproportionation reaction [13] suggest that the kinetic properties of Pu(V) are central to the behavior of Pu in aqueous media. It has long been maintained that the persistence of Pu(V) in natural waters with near neutral pH is due to a strong dependence of the reaction rate on the [H^+]. Choppin [31] states that the disproportionation reaction depends on the square of the Pu(V) concentration and on the fourth power of the [H^+]. This conclusion is apparently based on the following formulation of the disproportionation reaction:

$$2PuO_2^+\ (aq) + 4H^+\ (aq) \rightarrow PuO_2^{2+}\ (aq) + Pu^{4+}\ (aq). \tag{9}$$

With such a high dependence on [H^+], one would expect that disproportionation of Pu(V) at near-neutral pH would be immeasurably slow. This assessment is not supported by experimental measurements showing that the rate of Pu(V) disappearance is proportional to [H^+] at pH 0–1 [37]. The behavior at pH 0–1 is consistent with a mechanism involving protonation of PuO_2^+ and reaction of the $PuO(OH)^{2+}$ product in the rate-determining electron-transfer step.

Eq. (8) describes the net result of the disproportionation reaction associated with transfer of an electron between two Pu(V) ions. Electron transfer requires association or dimerization of two Pu(V) ions and is probably the rate-determining process. Regardless of the mechanism, formation of Pu(IV) and Pu(VI) in solution ultimately results in formation of products as described by Eq. (8). Spectroscopic data show that Pu(V) at an initial concentration of 10^{-2} M in $HClO_4$ solution at pH 1.5–2 disproportionates over a period of months [23]. The decrease in [Pu(V)] is accompanied by accumulation of Pu(VI) in solution and formation of an amorphous solid identified as colloidal PuO_2. Likewise, disproportionation of 10^{-3} M Pu(V) in chloride brine at pH 7.1 is indicated by accumulation of Pu(VI) in solution and precipitation of an unidentified solid [24].

The fate of Pu(VI) formed from the disproportionation of Pu(V) is uncertain because the proposed reduction of Pu(VI) by radiolytic H_2O_2 [13] is not supported by more recent experimental observation. Spectroscopic [Pu(VI)]-time data measured after addition of ^{239}Pu(VI) to a solution at pH 1.5 [23] and after addition of ^{242}Pu to high-purity water at pH 6 [38] show that Pu(VI) disappears at a progressively slower rate over time. Behavior parallels that for Pu(V) and suggests that d[Pu(VI)]/dt is a function of [Pu(VI)]. Development of a kinetic model in this study depends on accurate rate data for disappearance of Pu(V) and Pu(VI).

Rate-concentration results derived from analytical data for Pu(V) (open symbols) and Pu(VI) (solid symbols) in Fig. 3 show linear $\ln(d[Pu]/dt)$–$\ln[Pu]$ relationships defined by lines with ideal slopes of 2. Therefore, disappearance rates of both Pu(V) and Pu(VI) are described by the same general equations over the pH 0–7 range.

$$d[Pu]/dt = k[Pu]^2. \tag{10}$$

The line without data points describes the dependence of $d[Pu(V)]/dt$ on [Pu(V)] at pH 0 reported by Rabideau [37]. Results derived from spectroscopic data show that the rate equations for Pu(V) (open circles) and Pu(VI) (solid circles) at pH 1.5 are indistinguishable [23]. Results derived from radiometric analysis of [Pu] in brine at pH 7.1 (open triangles) are consistent with spectroscopic results, but may be slightly in error because data are not corrected for ingrowth of other oxidation states. Values of rate constants, k, derived from results in Fig. 3, are given in Table 1. Comparison of the data for pH 0 and pH 1.5 rate constants for Pu(V) in $HClO_4$ appears to exclude a dependence of the disproportionation rate on the fourth power of the H^+ concentration.

We do not have data to identify the products formed when Pu(VI) disappears from solution; however, dependence of $d[Pu(VI)]/dt$ on the square of [Pu(VI)] would be consistent with disproportionation of Pu(VI) into Pu(V) and Pu(VII) as the primary pathway for disappearance. In addition to the data at pH 1.5, observations (Fig. 3) based on spectroscopic results for

Table 1
Rate constants for disproportionation of Pu(V) and the disappearance of Pu(VI)[a,b] from solution

Oxidation state	Solution[c]	pH	k (l/mol s)
Pu(V)	$HClO_4$	0	6.3×10^{-3}
Pu(V)	$HClO_4$	1.5	5.2×10^{-5}
Pu(V)	2.5 M Cl^-, 0.82 mM HCO_3^-	7.1	0.42
Pu(VI)	$HClO_4$	1.5	5.2×10^{-5}
Pu(VI)	High-purity H_2O, ^{242}Pu	6	2.1×10^{-3}
Pu(VI)	2.5 M Cl^-, 0.82 mM HCO_3^-	7.1	6.3×10^{-4}

[a] Results are derived using data from literature sources [23,24,38].
[b] The rate equation for both oxidation states is $d[Pu]/dt = k[Pu]^2$.
[c] Except where noted, Pu is present primarily as the 239 isotope.

^{242}Pu(VI) in high-purity water at pH 6 (solid inverted triangles) [38] and on radiometric results for Pu(VI) in 2.5 M chloride solution at pH 7.1 (solid squares) [24] are consistent with this reaction. The k value for ^{242}Pu(VI) ($t_{1/2} = 3.8 \times 10^5$ y) exceeds those for ^{239}Pu(VI) ($t_{1/2} = 2.4 \times 10^4$ y), suggesting that reactions involving radiolytic products such as H_2O_2 are not the dominant process at the Pu concentrations present in the test solutions. If disproportionation of Pu(VI) is the mechanism for its disappearance, it is followed by rapid spontaneous reaction of Pu(VII) with H_2O to reform Pu(VI) [39]. An earlier proposal that an alpha-induced reaction of PuO_2^{2+} (aq) with water produces PuO_2^+ (aq) plus H^+ and 1/4 O_2 (g) [13] seems unlikely. In general, the most active species produced by radiolysis reactions are oxidants, while the dominant reducing agent is H_2, a relatively unreactive species.

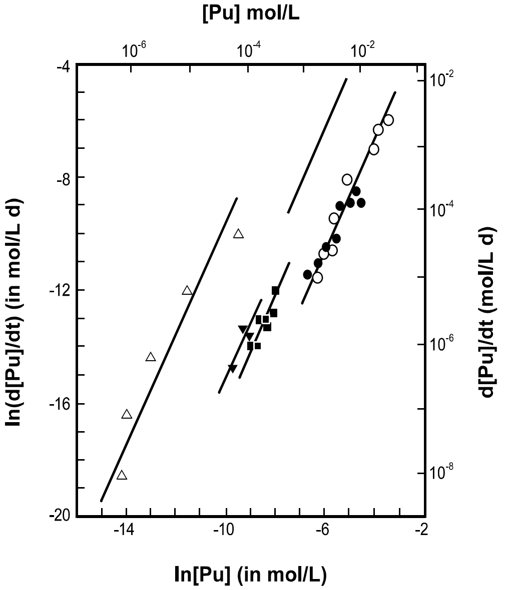

Fig. 3. Dependence of ln d[Pu]/dt on ln[Pu] for Pu(V) (open symbols and line with no symbols) and Pu(VI) (solid symbols) in differing solutions. The line without data is based on a published rate equation [37]; data are derived from analytical results in literature sources as follows: circles [23], upright triangles [24], squares [24], and inverted triangles [38].

3. Conceptual and quantitative kinetic models

The material presented in Section 2 shows that a dissolution model based solely on equilibrium thermodynamics and solubility of PuO_2 or $Pu(OH)_4$ is not consistent with the experimental data. A comprehensive model must be consistent with all observations:

(1) The [Pu] increases after precipitation of $Pu(OH)_4$ (am) from a solution oversaturated with Pu^{4+} (aq).
(2) Observed steady-state Pu concentrations for both PuO_2 and $Pu(OH)_4$ are higher than predicted for equilibrium systems.
(3) The steady-state [Pu] observed in dissolution studies with PuO_2 is about 10^2 less than that observed with $Pu(OH)_4$ (am).
(4) The slope of log[Pu] versus pH data is −1.
(5) The steady-state [Pu] is apparently insensitivity to *Eh*.
(6) The steady-state [Pu] depends on the amount of solid present.
(7) High mole fractions of Pu(VI) are found in steady-state solutions.
(8) Solids formed in the solutions have a CaF_2-related structure and lattice parameters exceeding that of PuO_2.
(9) Initially crystalline PuO_2 exposed to low pH shows a steady-state [Pu] coincident with that of $Pu(OH)_4$ after separation and exposure to new solutions at higher pH.
(10) Identical green steady-state solids form regardless of the initial Pu source [29].
(11) Extensive digestion of the solid is observed, especially at low pH [2,22].

These observations support a kinetically controlled chemical process involving release of Pu(V) from PuO_{2+x} formed by spontaneous reaction of dioxide or hydroxide with water.

Explanations of some of the observations listed above have been proposed, but these are frequently inconsistent with the conditions of the experiments. For example, higher-than-expected Pu concentrations and the increase in [Pu] after precipitation of $Pu(OH)_4$ might result from colloid formation. That possibility is not consistent with careful use of filtration methods during measurements or with the observation of high steady-state Pu(V) and Pu(VI) concentrations. Likewise, occurrence of a process based on disproportionation of Pu(IV) into Pu(III) and Pu(VI) [13] is also unlikely, since it should produce readily observable amounts of Pu(III), which are not observed.

3.1. The conceptual model

Spontaneous formation of green PuO_{2+x} by the PuO_2–H_2O reaction and identical rates for formation of Pu(V) in the higher oxide and for dissolution of plutonium dioxide are key observations suggesting that the steady-state Pu concentration is controlled by the rate at which Pu(V) forms and enters solution. Support for this approach is strengthened because leaching of Pu(V) as PuO_2^+ (aq) accounts for the −1 slope of log[Pu] − pH and disproportionation of PuO_2^+ (aq) provides an *Eh*-independent pathway to high PuO_2^{2+} (aq) concentrations. Involvement of the higher oxide is also suggested by formation of CaF_2-related steady-state solids with lattice parameters corresponding to those of PuO_{2+x}, a phase that is expected to have higher solubility than $Pu(OH)_4$ (am). Since the oxidation rate and the dissolution rate of a solid are surface-area dependant, [Pu] increases as PuO_{2+x} forms over a period of weeks after precipitation of $Pu(OH)_4$ (am) and the steady-state [Pu] depends on the amount and effective surface area of PuO_{2+x} present in the system.

A kinetically controlled process initiates with Pu(V) formation in PuO_{2+x} and leaching of Pu(V) into solution. Pu(V) disproportionates with formation of Pu(VI) and precipitation of Pu(IV) as hydrous oxide. Kinetics of the disproportionation process determine the steady-state concentrations of Pu(V) and Pu(VI) and the concentration of Pu(IV) is fixed by equilibrium with $Pu(OH)_4$ (am). Pu ions in solution at steady-state equilibrate with complexes and adsorbates. Transformation of hydroxide into oxide completes the process. Each of the four steps in the process is observed independently. Oxidation of PuO_2 to PuO_{2+x} is demonstrated [1] and dissolution of Pu as PuO_2^+ (aq) [26,31] has been proposed to explain experimental observations. Reduction of Pu(V) and Pu(VI) at pH 1.5 [23] and Pu(VI) at pH 6 [38] occurs over a period of months to years in solutions without addition of reducing agents. Amorphous hydroxide transforms into a CaF_2-related, steady-state solid consistent with PuO_{2+x} [25,34].

3.1.1. Formation of Pu(V) in PuO_{2+x} and leaching of Pu(V)

The proposed model includes formation of PuO_{2+x} as the stable steady-state solid in solution. Since the tetrahydroxide spontaneously transforms into dioxide, PuO_2 and $Pu(OH)_4$ both react with water to form PuO_{2+x}. Formation of PuO_{2+x} is expected to increase the rate of dissolution and solubility of the oxide.

Properties of PuO_{2+x} correspond to those of the less crystalline oxide identified in an earlier study [22]. XRD results show that the steady-state value of x varies from 0 near pH 10 to 0.5 near pH 3 if a linear x–pH dependence is assumed. This pH range corresponds to Region C in Fig. 2 and suggests that PuO_{2+x} is the coexisting solid at steady state. The reaction is consistent with the low *Eh* values in Region III of Fig. 2 because dissolved O_2 is preferentially consumed by PuO_{2+x} formation. The low *Eh* values measured in steady-state solutions at pH 4–9 do not influence the dissolution process; they are a consequence of the spontaneous chemical reaction that forms PuO_{2+x}. This conclusion is supported by coincidence of the sharp *Eh* increase with the pH at which the maximum PuO_{2+x} composition is reached. *Eh* increases at low pH because oxygen is not scavenged after the $PuO_{2.5}$ composition is reached near pH 3.

Dissolution of oxide is a two-step process involving formation of Pu(V) in the solid and removal of PuO_2^+ (aq) to the solution. The initial step is given by Eq. (1). The Pu(V) present in the solid solution of Pu(IV) and Pu(V) in PuO_{2+x} can then be preferentially removed into solution. The process is analogous to the preferential leaching of U(VI) from UO_{2+x} [19]. The process of oxidation of Pu(IV) to Pu(V) creates oxygen deficiency in the solid, while the dissolution of Pu(V) as PuO_2^+ (aq) creates a balancing excess of oxygen in the solid. The net process can be expressed as

$$y(\mathrm{PuO}_{2+x}) + \mathrm{H}^+(\mathrm{aq}) \rightarrow \mathrm{PuO}^+(\mathrm{aq}) + (y-1)(\mathrm{PuO}_{2+x}) + x\mathrm{O}(\text{in } \mathrm{PuO}_{2+x}) + 1/2\mathrm{H}_2(\mathrm{g}). \tag{11}$$

3.1.2. Disproportionation of Pu(V) and Pu(VI)

The proposed model depends on the solution chemistry of PuO_2^+ (aq); as indicated by Eq. (8), PuO_2^+ (aq) disproportionates into Pu(VI) (aq) and Pu(IV) (aq). $Pu(OH)_4$ (am) precipitates after its solubility product is exceeded and PuO_2^{2+} (aq) accumulates in solution until its rate of reduction equals the rate of its formation. That accumulation of Pu(VI) accounts for the persistent presence of Pu(VI) in solution at steady state.

To prevent excessive accumulation of Pu(VI) in solution, there must be some process to reduce Pu(VI). Alpha-induced reduction has been proposed as the driver for Pu(IV) formation in solutions containing Pu(VI)

[23,38]; however, this explanation is inconsistent with experimental evidence. Although the specific activity of ^{239}Pu exceeds that of ^{242}Pu by a factor of 15, the most rapid rate of Pu(VI) disappearance at a given [Pu(VI)] is observed for the 242 isotope in high-purity water (Table 1). As implied by the dependence of $\mathrm{d}[\mathrm{Pu(VI)}]/\mathrm{d}t$ on the second power of [Pu(VI)], a more likely explanation is that Pu(VI) disproportionates to Pu(V) and highly reactive Pu(VII) via an electron-transfer reaction.

3.1.3. The conceptual kinetic model

A chemical process involving several Pu oxidation states accounts for the continuous digestion and redistribution of the solid over time and for the failure of the system to display equilibrium behavior [2]. Existence of the process is implied by attainment of essentially identical steady-state Pu concentrations, oxidation state distributions, and coexisting solids, regardless of the initial chemical state of the system.

As defined by x in the formula PuO_{2+x}, the concentration of Pu(V) in the oxide increases at a fixed rate as the oxide–water reaction proceeds at constant temperature for a given pH. The leaching rate of Pu(V) increases with increasing x. In an equilibrium system, the equilibrium values of x and PuO_2^+ (aq) are ultimately reached regardless of the rates at which Pu(V) forms or leaches. With plutonium oxide, the equilibrium state is never reached because PuO_2^+ (aq) is kinetically unstable and disproportionates at an increasingly rapid rate as it accumulates in solution. Consequently, x increases until the leach rate equals the rate of Pu(V) formation and a steady state is established. As outlined in Table 2, this condition leads to the sequence of steps that determines the equilibrium concentration of Pu(IV) and the steady-state concentrations of Pu(V) and Pu(VI) in solution.

The initial reaction of PuO_2 with water to form PuO_{2+x} occurs spontaneously at room temperature, driven in part by the large entropy increase when liquid water is consumed and hydrogen gas is formed. The disproportionation reaction of Pu(V) is known to occur spontaneously [13]. We do not have detailed knowledge of the process that results in the disappearance of Pu(VI) from solutions; however, it is seen from the data in Table 1 to be a spontaneous process. In the discussions that follow we will describe the process as disproportionation, but any process that depends of the square of the [Pu(VI)] will produce the same results in the model.

3.2. The quantitative kinetic model

Calculation of steady-state concentrations of Pu(V) and Pu(VI) is simple and limited only by availability of kinetic data and knowledge of the effective (chemically active) surface area of the solid in contact with the solution. The active surface area of the steady-state solid is needed to relate the area-dependent rate of Pu(V) formation in the solid to the volume-dependent rate of Pu(V) disproportionation in solution. At this time, application of the model is restricted to solutions near pH 7 because rate data are available only for Pu(V) formation in PuO_{2+x} at near-neutral conditions (Eq. 2). Kinetic data for disproportionation of Pu(V) and Pu(VI) at pH 7 are available for high-ionic-strength (2.5 M chloride brine) solutions (Table 1). The steady-state concentrations of Pu(V) and Pu(VI) are derived by substituting the formation rates of Pu(V) and Pu(VI) into the respective rate equations for disproportionation.

The steady-state [Pu] observed in studies with $Pu(OH)_4$ (am) is consistently comprised of more than 94% Pu(V) + Pu(VI) at pH 7 and the ratio of Pu(VI) to Pu(V) increases from 0.5 ± 0.2 in low-ionic-strength solution to 7 ± 1 in 2.5 M chloride solution [2]. In a similar way, use of PuO_2 microspheres instead of $Pu(OH)_4$ (am) as the initial solid in low-ionic-strength solutions at pH 7 is accompanied by an increase in the steady-state Pu(VI) percentage from $33 \pm 14\%$ to 95%. These changes afford opportunities for quantitatively testing the proposed model, but the rate equation for Pu(V) disproportionation is not known at pH 7 for low

Table 2
Sequence of kinetic and equilibrium processes occurring in a steady-state solution containing plutonium oxide or hydroxide at constant pH

1	Pu(V) accumulates in PuO_{2+x} as x is increased by spontaneous reaction of PuO_2 with H_2O[a]
2	The rate of PuO_2^+ dissolution increases with increasing x in PuO_{2+x} until it equals the rate of Pu(V) formation and a steady state is established
3	PuO_2^+ accumulates until its rate of disproportionation into PuO_2^{2+} and Pu(IV) equals its rate of entry into solution and a steady state is established
4	PuO_2^{2+} accumulates until disproportionation and reduction reform PuO_2^{2+} at a rate equal to half the PuO_2^+ dissolution rate and a steady state is established
5	Pu(IV) accumulates until its concentration satisfies the K_{sp} for $Pu(OH)_4$ precipitation and the equilibrium Pu(IV) concentration of 1×10^{-9} M Pu(IV) is established
6	Metastable $Pu(OH)_4$ spontaneously transforms into PuO_2 and subsequently back to PuO_{2+x}

[a] This reaction produces hydrogen gas, which escapes from the system. This means the Pu cycle is not an equilibrium process, but achieves a steady-state situation as long as the supply of water is not exhausted.

ionic-strength solutions (Table 1). Therefore, use of an alternative kinetic equation is necessary to relate the rate of Pu(V) disappearance to the Pu(V) concentration in near-neutral (pH 6–7) solution at low ionic strength.

A kinetic equation described by Rabideau and Kline [40] relates the rate of Pu(V) disappearance in $HClO_4$ solution at low pH to the concentrations of Pu(V) and other oxidation states.

$$\mathrm{d}[\mathrm{Pu(V)}]/\mathrm{d}t = k_{\mathrm{IV,V}}[\mathrm{Pu(IV)}][\mathrm{Pu(V)}] - k_{\mathrm{III,VI}}[\mathrm{Pu(III)}][\mathrm{Pu(VI)}]. \tag{12}$$

The second term of the equation is ignored because the [Pu(III)] is negligibly small at steady state. The rate constant, $k_{\mathrm{IV,V}}$, is a function of pH and its dependence on $[\mathrm{H}^+]$ is defined by regression analysis of published data.

$$k_{\mathrm{IV,V}}\ (\mathrm{l/mol\,Pu(V)\,s}) = (35.5 \pm 2.5)[\mathrm{H}^+]^{0.13\pm0.05}. \tag{13}$$

The value of $k_{\mathrm{IV,V}}$ at pH 6.5 is 5.0 l/mol s and the concentration of Pu(IV) in equilibrium with $Pu(OH)_4$ (am) is 1×10^{-9} mol/l at pH 6–7 [2,25]. Use of the equilibrium [Pu(IV)] in defining kinetic behavior directly involves the equilibrium process for $Pu(OH)_4$ (am) (step 5 in Table 2) in the kinetic calculation of [Pu(V)] at steady state.

Derivation of the areal-volumetric conversion factor, C, is complicated by lack of knowledge about properties of the solid(s) present at steady state. A difference in surface area exists initially if the starting solid is $Pu(OH)_4$ (am) precipitate instead of PuO_2 microspheres. The precipitate may behave like a finely divided powder with a high specific area or like a gelatinous mass with the limited surface area of a massive solid. In addition, C depends on the fraction of area that is active PuO_{2+x}. That fraction may be small and is likely to be reduced by precipitation of fresh $Pu(OH)_4$ (am) on solid surfaces. Fine PuO_2 powders have specific surface areas on the order of 50 m^2/g [41] and a value of 100 m^2/g is adopted as a reasonable value for high-surface-area hydroxide. For typical test solutions with initial Pu concentrations on the order of 10^{-4} M (0.03 g $Pu(OH)_4$/l), the estimated maximum C is about 3 m^2/l if the entire surface is PuO_{2+x}. If the hydroxide acts like a solid mass on the bottom of a 1 l container, the area is approximately 100 cm^2, a value that does not vary significantly with the amount of solid present. In this case, C for a fully active surface is approximately 0.01 m^2/l. Estimation of C is easier for studies with PuO_2 microspheres, which are typically several hundred micrometers in size. The calculated specific area of microspheres with diameters of 500 μm is about 0.001 m^2/g. If the oxide surface is fully active, C for experiments with 0.4 g PuO_2/l [30] is 0.0004 m^2/l.

Derivation of C using kinetic data and assumptions of the model suggests that the fraction of active surface is small. If a steady state is established, the product of the areal rate, R, for Pu(V) formation in PuO_{2+x} (Eq. (2)) and C is twice the volumetric rate for disproportionation of Pu(VI) at pH 7 (Table 1). R is about 1×10^{-13} mol Pu(V)/m^2 s and the value of $\mathrm{d}[\mathrm{Pu(VI)}]/\mathrm{d}t$ ($\sim 1 \times 10^{-17}$ mol Pu/l s) is derived using the steady-state [Pu] (1×10^{-7} mol Pu/l) for $Pu(OH)_4$ at pH 7 (Fig. 2) and k ($\sim 1 \times 10^{-3}$ l/mol s) for pH 7 (Table 1). The calculated C ($\sim$0.0002 m^2/l) is substantially less than estimated values for a fully active surface.

Steady-state concentrations of Pu(V) and Pu(VI) are calculated using Eq. (10), rate constants for disproportionation of Pu(V) and Pu(VI) in Table 1, and the rate, R, of Pu(V) formation in PuO_{2+x} at 25 °C.

$$[\mathrm{Pu}] = ((\mathrm{d}[\mathrm{Pu}]/\mathrm{d}t)/k)^{1/2} = (CR/k)^{1/2}. \tag{14}$$

In all calculations, R for Pu(V) is 1×10^{-13} mol Pu(V)/m^2 s and R for Pu(VI) (5×10^{-14} mol Pu(VI)/m^2 s) is half that of Pu(V). The k values for Pu(V) and Pu(VI) are 0.42 and 0.0063 l/mol s, respectively (Table 1). Results of steady-state calculations for 2.5 M chloride brine at pH 7 using selected C values within the estimated range (0.0002–3 m^2/l) are compared with experimental results in Table 3.

Parallel calculations for low-ionic-strength solutions at near-neutral pH involve Eqs. (12) and (13). Elimination of the second term in Eq. (12), rearrangement, and inclusion of R and C give the equation for calculating the steady-state [Pu(V)].

$$[\mathrm{Pu(V)}] = (\mathrm{d}[\mathrm{Pu(V)}]/\mathrm{d}t)/k_{\mathrm{IV,V}}[\mathrm{Pu(IV)}] = (CR)/k_{\mathrm{IV,V}}[\mathrm{Pu(IV)}]. \tag{15}$$

Since the [Pu(IV)] is available from equilibrium modeling, Eq. (15) is applicable for studies with both PuO_2 (s) microspheres and $Pu(OH)_4$ (am), but different values of C apply as indicated in Table 3.

Agreement of the calculated and observed steady-state Pu concentrations and oxidation-state distributions is good. The effects of high chloride concentration and low PuO_2 surface area are reflected in prediction of high steady-state percentages of Pu(VI). Concentrations calculated with large values of C consistently exceed the observed steady-state [Pu], suggesting that only a small fraction of the solid surface is active. The difference in values of C for oxide microspheres and amorphous hydroxide accounts for the factor of 10^2 between observed steady-state Pu concentrations for those solids (Fig. 1) and implies that the difference is a direct consequence of the active area of the solid in contact with the solution. Digestion of PuO_2 microspheres at low pH produces a high-surface-area solid similar to that obtained by hydroxide precipitation and results obtained in further tests at high pH are indistinguishable from those with $Pu(OH)_4$ (am) [30].

Table 3
Comparison of predicted Pu concentrations and oxidation-state distributions with experimental results

Conditions	C	log[Pu]	%Pu(IV)	%Pu(V)	%Pu(VI)	Reference
$Pu(OH)_4$ (am), pH 7, 2.5 M Cl^-	0.1	−5.5	0.03	5	95	
	0.01	−6.0	0.1	5	95	
	0.005	−6.1	0.1	5	95	
	Obs.	−7.5 to −6.1	1–5	5–28	70–96	[24]
$Pu(OH)_4$ (am) pH 6–7, low I	0.1	−5.5	0.03	67	33	
	0.01	−6.1	0.1	31	69	
	0.005	−6.3	0.1	24	76	
	Obs.	−5.5 to −7.4	0.3–6	39–73	18–59	[20,29]
PuO_2 (s) microspheres pH 7, low I	0.0004	−7.0	1	7	92	
	0.0002	−7.1	1	6	93	
	Obs.	−7.5 to −8.1	5	0	95	[30]

4. Pyrochemical salts

Pyrochemical salt wastes were produced during processing of weapons Pu at the Rocky Flats Plant in Colorado over a 25 year period. The residues are primarily solidified chloride salts used as molten solvents in several processes including direct oxide reduction (DOR) of PuO_2 to metal, molten salt extraction (MSE) of Am from Pu metal, and molten salt electrorefining (ER) of impure plutonium metal. The DOR process used $CaCl_2$, while MSE and ER used mixtures of NaCl–KCl or NaCl–$CaCl_2$. In addition to metallic Pu that did not coalesce into the product pool during processing, Mg metal may be present in MSE salts and Ca metal may be present in DOR salts. Characterization of ER residues showed Pu concentrations of 10 ± 5 percent by weight, primarily as 1 mm diameter metal spheres embedded in the salt. Partial oxidization of Pu during storage is attributed to the presence of water of hydration that sharply accelerates the rate of oxidation compared to dry conditions and produced corrosion layers of 200–400 μm thickness after less than 10 years in storage [42,43].

The US Department of Energy is disposing of pyrochemical salt wastes at the WIPP facility in Carlsbad, NM. The wastes are packaged in 12 in. (30.5 cm) diameter by 24 in. (61 cm) long stainless steel pipes (Pipe Overpacks, POCs) with a volume of 44 l. The pipes are packed into 55 gallon (208 l) drums filled with shock-absorbing material. The maximum concentration of Pu in each package is 180 g Pu/POC, while the average concentration of the first 3374 POCs (out of a planned total of 6104) was 140 g Pu/POC [44].

The expected behavior of Pu under WIPP disposal conditions was estimated using equilibrium thermodynamic calculations for the chemistry of Th as an analog for Pu [45]. No samples of pyrochemical salt wastes from Rocky Flats were tested to determine the release of Pu from these wastes in brines representative of those expected for WIPP conditions. Some testing was done, however, on pyrochemical salt samples produced at Los Alamos National Laboratory (LANL) by chemical methods similar to those used at Rocky Flats. Results from some of those tests are discussed below and compared to the expectations from equilibrium thermodynamic modelling calculations and from the conceptual kinetic model for Pu solution chemistry control discussed in Section 3.1.3.

4.1. Behavior of pyrochemical salt wastes in brines

Two types of brines are expected to be important with respect to interaction with waste at the WIPP facility: the Salado formation brine, which is present in the repository-level salt formation, and the Castile brine, which comes from an underlying salt bed. The Salado brine contains 1.44 M Mg^{2+}, 1.83 M Na^+, and 0.7 M K^+ with Cl^- as the dominant anion (5.35 M), while the Castile brine is essentially 4.8 M NaCl with minor impurities. A synthetic version of the Salado brine used in testing was called ‘Brine A’ [45, Appendix SOTERM].

The DOE supported a multi-year program of tests at LANL under the title ‘The Actinide Source-Term Waste Test Program’ (STTP). Results of STTP tests have not been published in a formal way, but have been released in viewgraph form at meetings involving DOE, Environmental Protection Agency, and Environmental Evaluation Group personnel and consultants. In addition, a DOE ‘White Paper’ concerning tests that showed evidence for Pu(VI) in the brine solution has been distributed on at least two occasions [46].

The STTP tests were conducted in 3 l Ti vessels using approximately 1.32 kg of DOR salts with about 1.7 l of brine. Each test included 110 g Fe mesh, 45 mg of Nd, and 75 mg each of Th, U, and Np. Test L26 used Brine A and contained 3.09 g total Pu plus 1.71 mg ^{241}Am, while test L27 used Castile brine and contained 3.57 g total Pu with 1.55 mg ^{241}Am. During the test period from March 1995 to May 1999 pcH in Brine A was about 8, while pcH in Castile brine was about 11.

The STTP test data show the following general features. Solution concentrations of Pu rose gradually in the case of L26 and more rapidly for L27 to maxima after 20 months of 71 ppm for L26 and 243 ppm after 7 months for L27. The peak concentration for L27 was about three times higher than for L26, although the tests reportedly contained similar amounts of total Pu. After peaking, [Pu] gradually decreased and apparently approached a steady-state value of about 4 ppm (1.7×10^{-5} M) for L26 and 25–30 ppm for L27. Test L25, which contained only 10% as much Pu as L26, but was conducted in Brine A and should otherwise be similar to L26, had a peak concentration of only 0.17 ppm and a final concentration of 0.06 ppm (3×10^{-7} M), suggesting that the amount of Pu in the system strongly influences the steady-state concentration of Pu. The plutonium concentrations in these tests are much higher than those expected based on equilibrium thermodynamic calculations and point to a mechanism other than thermodynamic equilibrium solubility for control of Pu concentration.

The Fe mesh in the tests was expected to ensure reducing conditions and to favor Pu species in the Pu(III) and Pu(IV) valence states. The concentrations of Fe in solution samples were far higher than could be attributed to Fe(III) species, so the data indicate that reducing conditions were achieved. For test L26, the concentration of Fe in solution, [Fe], was relatively low (<1 ppm) throughout the test and only twice exceeded 4 ppm, while for test L27, the [Fe] at the first sampling time was 43 ppm. For test L27, the increase and subsequent decrease in [Pu] was mirrored in the behavior of Fe, which reached a peak of 243 ppm after 1 year.

The speciation of Pu in the test samples was measured using UV–visible spectroscopy, a method that requires rather high concentrations in solution for positive identification of Pu(V) and Pu(VI). The first spectroscopic results for L27 were obtained at the end of December 1996 and recorded the presence of Pu(V) in a solution that contained 87 ppm Pu. In late March 1997, sample L26 had a [Pu] of 63 ppm and showed the presence of Pu(VI), but not Pu(V). The sample taken for L27 at that time had [Pu] = 44 ppm and showed the presence of Pu(V) but no Pu(VI). Test L26 continued to show Pu(VI) until the concentration of Pu dropped below 10 ppm in late 1998, while the L27 samples continued to show Pu(V) without Pu(VI) until the concentrations dropped to less than 30 ppm.

To understand the spectroscopy data, we must discuss the detection limits for Pu valence states in the two brines. The detection limit for Pu(V) in Brine A is >0.5 mM, a [Pu] corresponding to a solution concentration of 120 ppm (5×10^{-4} M). Thus, all results for Pu in test L26 in Brine A apparently had concentrations below the detection limits for Pu(V). If the assumed detection limit for Pu(V) in Castile brine is about 24 ppm, a value somewhat lower than the last positive identification of Pu(V) in samples from L27, this would be 0.1 mM. Spectroscopic detection limits for Pu(VI) in brines are much lower than for Pu(V). The detection limit for Pu(VI) in Castile brine is about 0.01 mM, which limits the [Pu(VI)] in the L27 tests to less than 2.4 ppm. Spectroscopic data for L26 show that Pu(VI) is not detectable below 9 ppm, corresponding to a detection limit of about 3×10^{-5} M for Pu(VI) in Brine A if only that oxidation state is present.

4.2. Interpretation of STTP test data

The STTP tests contain metallic Fe and Fe(II) ions in the brines as well as the likely presence of metallic Pu at the start of the tests. The conceptual model for Pu solubility presented in Section 3.1.3 is valid only if Pu is present as oxide or hydroxide. We can, however, use the concepts in the model to help provide an interpretation for the pattern of data found. Iron mesh that was included in the tests provided a means of adding reducing agents to the system. Reduction of Pu(V) and Pu(VI) to lower oxidation states increases the steady-state [Pu] and alters the distribution of oxidation states, but the presence of Fe does not eliminate Pu(V) and Pu(VI) from a brine at steady state.

The transient effects caused by initial presence of Pu metal can be estimated from studies of the corrosion of Pu metal, which was described in Section 2.1. Studies in 1 M $CaCl_2$ gave PuOH as the initial product [4]. The [Pu] coexisting with this phase has been shown to be 1.4×10^{-5} M [47]. The PuO_{2+x} product formed after approximately one year is a finely divided solid (7 nm average particle size) and is the stable oxide in chloride-rich solutions, as well as in low-ionic-strength waters [4]. Appearance of time-dependent maxima in [Pu] for the L26 and L27 tests is consistent with formation of relatively soluble intermediate phases during oxidation of Pu to PuO_{2+x}. Solubility data are available only for PuOH and correspond to a concentration less than the maxima found in L26 and L27. The apparent time periods (2.5–3.5 years) for establishing steady states in brine tests are longer than those found in low ionic strength solubility studies, and may reflect the kinetic effects of high Cl^- concentration and the presence of Fe. Brine composition may also influence the reaction rates and mechanisms. Salado brine is thought to develop reaction layers on some materials and impede their corrosion. This may explain the low [Fe] in the Salado brine and the relatively high [Fe] in the Castile brine. Detection of only Pu(V) in the L27 test is consistent with a high [Fe] that is presumably present as Fe(II) and prevents accumulation of Pu(VI) in solution.

4.3. Data needs for development of a quantitative model for brines

In order to understand the behavior of plutonium in aqueous solutions, one must be able to analyze both the concentration of total Pu and the distribution of oxidation states of Pu as the system develops through time. Methods commonly used in studying Pu chemistry employ solvent extraction techniques to separate Pu(III + IV) from Pu(V + VI) as was done in the study by Rai et al. [26]. Schemes based on organic extractions that allow determination of each of these four valence states using a number of extractions have been used in some studies [24], but are generally not employed because they are very time-consuming. UV–visible spectroscopy can be used to detect Pu(V) and Pu(VI), but only at high concentrations. Development of analytical methods that allow rapid separation of the different valence states of Pu followed by quantitative analysis at low concentrations is needed. The method developed by Röllin [48], which used a rapid separation of actinides with different valence states followed by ICP–MS analysis, is an example of the type of technique that needs to be used.

The kinetic model for Pu solution evolution requires three basic rate constants, each of which may be a function of pH and [Cl$^-$]. In addition, the presence of reducing agents such as Fe metal or Fe(II) ions may affect the reaction rates and the steady-state [Pu] concentration. Execution of a complete experimental matrix to cover all parameter ranges would be a very large effort; however, the task can be reduced to manageable proportions with suitable selection of parameters from a limited range that is applicable to waste disposal needs. The basic parameters that are needed are:

(1) the rate of Pu(V) production in Pu(OH)$_4$ as a function of [NaCl] and pH;
(2) the rate of disappearance of Pu(V) from solution as a function of [NaCl] and pH; and
(3) the rate of disappearance of Pu(VI) from solution as a function of [NaCl] and pH.

Data for items (2) and (3) exist at pH 7.1 and [NaCl] = 2.4 M. If data were produced for [NaCl] = 0.1 and 4.8 M at pH 7.1, the chloride dependence of these reaction rates could be evaluated. If the dependence of rates on [NaCl] is not too great, the pH dependence of the rates could be evaluated at a single [NaCl], for example 2.4 M. Tests at pH 9 and 11, together with the existing data at pH 7.1, would give the pH dependence of the rates. The effect of Fe could be evaluated initially by using a single pH and [NaCl] together with two experimental conditions – one with an initial concentration of Fe(II) without a replenishment source and one with an actively corroding piece of Fe metal to provide a constant source of Fe(II) ions. A similar experimental matrix for the oxidation of Pu(OH)$_4$ as a function of [NaCl] and pH would complete the reaction rate data needs. If any of the reaction rates turned out to be a sensitive function of one of the experimental parameters, more detailed studies could be planned.

For application of the model to waste disposal conditions, an estimate of the active surface area of the waste form Pu under disposal conditions is needed. If all of the rate constant data are available, an experiment could be conducted using an actual waste form and the fraction of active surface area could be calculated using the model and the experimentally determined [Pu] and valence state distributions. To validate the model, a second experiment using a different amount of waste material could then be conducted and the results of the experiment compared to the predictions of the model.

5. Conclusions

A model to describe the chemistry of Pu in solutions coexisting with plutonium oxide and hydroxide has been developed. The model is based on oxidation of PuO$_2$ by water to produce PuO$_{2+x}$ and release of Pu(V) to solution. The kinetic relationships between formation of PuO$_{2+x}$, dissolution of Pu(V), disproportionation of Pu(V) to Pu(IV) and Pu(VI), and reduction of Pu(VI) determine the steady-state concentrations of Pu(V) and Pu(VI) and the distribution of those valence states in solution. Complex formation in solutions with high chloride and carbonate concentrations may slow the Pu(VI) disproportion rate and shift the oxidation-state distribution toward the hexavalent state.

The total Pu concentration observed at steady state is a consequence of a hybrid kinetic-equilibrium process. The concentration and speciation of Pu(IV) are independently fixed at the equilibrium state determined by solution properties and the presence of Pu(OH)$_4$ (am). A non-equilibrium concentration of Pu(III) may be formed by reaction with Fe(II) (aq) or Fe metal. Predicted valence-state distributions for near-neutral solutions and steady-state Pu concentrations derived by summing concentrations of all species agree well with the results of dissolution experiments.

Additional experimental work is needed to verify the model and to establish a database of essential parameters. Before the model can be used for waste repository performance assessment, data are needed for solution conditions that are relevant to the specific repository. For the case of WIPP, data are needed for higher pH and for higher [Cl$^-$] than are presently available. The effect of Fe metal and Fe(II) ions on reaction rates must also be investigated.

Acknowledgements

This work was supported by the Environmental Evaluation Group. We are grateful for that support and the active interest in this work taken by Matthew Silva and Jim Channell. The manuscript was improved by revisions made after consideration of the review comments provided by Yngve Albinsson, Gunnar Skarnemark, and Hans Nilsson.

References

[1] J.M. Haschke, T.H. Allen, L.A. Morales, Science 287 (2000) 285.

[2] J.M. Haschke, R.L. Bassett, Radiochim. Acta, in press.

[3] J.M. Haschke, T.H. Allen, L.A. Morales, Los Alamos Sci. 26 (2000) 252.

[4] J.M. Haschke, Transuranium elements: a half century, in: L.R. Morss, J. Fuger, American Chemical Society, Washington, DC, 1992, p. 416.

[5] J.L. Stakebake, D.T. Larson, J.M. Haschke, J. Alloy Compd. 202 (1993) 251.

[6] J.M. Haschke, T.H. Allen, J.L. Stakebake, J. Alloy Compd. 243 (1996) 23.

[7] T.H. Allen, J.M. Haschke, Interaction of Plutonium Dioxide with Water and Oxygen–Hydrogen Mixtures, Los Alamos National Laboratory Report LA-13537-MS, 1999.

[8] L. A. Morales, J. M. Haschke, T.H. Allen, Kinetics of Reaction Between Plutonium Dioxide and Water at 25 °C to 350 °C: Formation and Properties of the PuO_{2+x} Phase, Los Alamos National Laboratory Report LA-13597-MS, 1999.

[9] J.M. Haschke, T.H. Allen, L.A. Morales, J. Alloy Compd. 314 (2001) 78.

[10] J.M. Haschke, T.H. Allen, J. Alloy Compd. 320 (2001) 58.

[11] L.R. Morss, Thermodynamic properties, in: J.J. Katz, G.T. Seaborg, L.R. Morss (Eds.), The Chemistry of the Actinide Elements, Vol. 2, Chapman and Hall, New York, 1986 (Chapter 17).

[12] M.H. Lloyd, R.G. Haire, Radiochim. Acta 25 (1978) 139.

[13] J.M. Cleveland, The Chemistry of Plutonium, American Nuclear Society, La Grange Park, IL, 1979.

[14] O.J. Wick (Ed.), Plutonium Handbook, American Nuclear Society, La Grange Park, IL, 1980 (Chapters 6, 8, 11, 12).

[15] F. Weigel, J.J. Katz, G.T. Seaborg, Plutonium, in: J.J. Katz, G.T. Seaborg, L.R. Morss (Eds.), The Chemistry of Actinide Elements, Vol. 1, Chapman and Hall, New York, 1986 (Chapter 7).

[16] J.M. Haschke, M.P. Sherman, J.L. Stakebake, Conceptual and Quantitative Models for Gas Generation During Transport and Storage of Plutonium Dioxide, Rocky Flats Report RFP-5390, 2001.

[17] J.M. Haschke, T.H. Allen, J. Alloy Compounds 336 (2002) 124.

[18] L.A. Morales, Presented at Plutonium Futures-The Science, Santa Fe, NM, 10–13 July 2000.

[19] D.W. Shoesmith, J. Nucl. Mater. 282 (2000) 1.

[20] H. Nitsche, R.C. Gatti, E.M. Sandifer, S.C. Lee, A. Müller, T. Prussin, R.S. Deinhammer, H. Maurer, K. Becraft, S. Leung, S.A. Carpenter, Report LA-12562-MS, Los Alamos National Laboratory, Los Alamos, NM, 1993.

[21] D. Rai, R.J. Serne, D.A. Moore, Soil Sci. Am. Soc. J. 44 (1980) 490.

[22] D. Rai, J.L. Ryan, Radiochim. Acta 30 (1982) 213.

[23] T.W. Newton, D.E. Hobart, P.D. Palmer, Radiochim. Acta 39 (1986) 139.

[24] H. Nitsche, K. Roberts, R. Xi, T. Prussin, K. Becraft, I.A. Mahamid, H.B. Silber, S.A. Carpenter, R.C. Gatti, C.F. Novak, Radiochim. Acta 66&67 (1994) 3.

[25] D.W. Efurd, W. Runde, J.C. Baner, D.R. Janecky, J.P. Kazuba, P.D. Palmer, F.R. Roensch, C.D. Tait, Environ. Sci. Technol. 32 (1998) 3893.

[26] D. Rai, D.A. Moore, A.F. Felmy, G.R. Choppin, R.C. Moore, Radiochim. Acta 89 (2001) 491.

[27] J.I. Kim, B. Kanellakopulos, Radiochim. Acta 48 (1989) 145.

[28] J.M. Haschke, T.E. Ricketts, J. Alloy Compd. 252 (1997) 148.

[29] H. Nitsche, N.M. Edelstein, Radiochim. Acta 39 (1985) 23.

[30] R.C. Dahlman, E.A. Bondietti, L.D. Eyeman, Amer. Chem. Soc. Symp. Ser. 35 (1976) 47.

[31] G.R. Choppin, in: V.M. Oversby, P.W. Brown (Eds.), Mater. Res. Soc. Proc., Vol. 176, Materials Research Society, Pittsburgh, PA, 1990, p. 449.

[32] D. Rai, Radiochim. Acta 35 (1984) 97.

[33] D. Rai, N.J. Hess, A.R. Felmy, D.A. Moore, M. Yui, P. Vitorage, Radiochim. Acta 86 (1999) 89.

[34] W. Runde, Unpublished data from studies described in Ref. [25], 2000.

[35] M.H. Rand, A.C. Fox, R.S. Street, Nature 195 (1962) 567.

[36] J.H. Patterson, G.B. Nelson, G.M. Matlack, The Dissolution of ^{238}Pu in Environmental and Biological Systems, Los Alamos Scientific Laboratory Report LA-5624, 1974.

[37] S.W. Rabideau, J. Am. Chem. Soc. 79 (1957) 6350.

[38] D.T. Reed, D.G. Wygmans, S.B. Aase, J.E. Banazak, Radiochim. Acta 82 (1998) 109.

[39] C. Keller, H. Seifert, Angew. Chem. Int. Ed. 8 (1969) 279.

[40] S.W. Rabideau, R.J. Kline, J. Am. Chem. Soc. 62 (1958) 617.

[41] J.M. Haschke, Plutonium Dioxide Storage: Conditions for Preparation and Handling, Los Alamos National Laboratory Report LA-12999-MS, 1995.

[42] J.M. Haschke, H.K. Fauske, A.G. Phillips, J. Nucl. Mater. 279 (2000) 127.

[43] J.M. Haschke, A.G. Philips, J. Nucl. Mater. 277 (2000) 175.

[44] M.K. Silva, Environmental Evaluation Group, Albuquerque, NM, personal communication, November 2001.

[45] US Department of Energy, Carlsbad Area Office, Title 40 CFR Part 191 Compliance Certification Application for the Waste Isolation Pilot Plant, Final. DOE/CAO-1996-2184 (21 vols.) 1996.

[46] No author given, The Observation of Plutonium in the +VI Oxidation State in the Actinide Source-Term Test Program Experiments, manuscript dated 23 March 2000 (p. 26). This manuscript was given to EEG on 19 April

2000. In addition, the manuscript was part of a package of material sent to EEG by EPA, received 19 March 2001.

[47] A.E. Hodges III, J.M. Haschke, Report RFP-2919, Rocky Flats Plant, Golden, CO, 1979.

[48] S. Röllin, On-line coupling of an ion chromatograph to the ICP–MS: separations with a cation exchange chromatography column, SKB Technical Report TR-99-35, Svensk Kärnbränslehantering AB, Stockholm, Sweden, December 1999.